Environmental Research 270 (2025) 121029

Contents lists available at ScienceDirect

Environmental Research

journal homepage: www.elsevier.com/locate/envres

Auto-induced uplink 4G and 5G RF-EMF exposure assessment using a network monitoring application in different microenvironments across seven European countries

Bram Stroobandt [a,*], Han Van Bladel [a], Adriana Fernandes Veludo [b,c], Kenneth Deprez [a], Sam Aerts [d], Leen Verloock [a], György Thuróczy [e], Piotr Politanski [f], Kinga Polanska [f], Gabriella Tognola [g], Marta Parazzini [g], Joe Wiart [h], Mònica Guxens [i,j,k,l,m], Martin Röösli [b,c], Wout Joseph [a]

[a] Ghent University - imec, Tech Lane Science Park 126, 9052, Ghent, Belgium
[b] Swiss Tropical and Public Health Institute (Swiss TPH), 4123, Allschwil, Switzerland
[c] University of Basel, 4001, Basel, Switzerland
[d] The Hague University of Applied Sciences, 2628 AL, Delft, the Netherlands
[e] National Center for Public Health and Pharmacy, Budapest, Hungary
[f] Nofer Institute of Occupational Medicine, Łódź, Poland
[g] Institute of Electronics, Information Engineering and Telecommunications (IEIIT), Consiglio Nazionale delle Ricerche, Milan, Italy
[h] Télécom Paris, Institut Polytechnique de Paris, Palaiseau, France
[i] ISGlobal, Barcelona, Spain
[j] Universitat Pompeu Fabra, Barcelona, Spain
[k] Spanish Consortium for Research on Epidemiology and Public Health (CIBERESP), Instituto de Salud Carlos III, Madrid, Spain
[l] Department of Child and Adolescent Psychiatry/Psychology, Erasmus MC, University Medical Centre, Rotterdam, the Netherlands
[m] ICREA, Barcelona, Spain

ARTICLE INFO

Keywords:
Uplink
Transmit power
4G
5G
Radiofrequency electromagnetic fields
Exposure
Microenvironments

ABSTRACT

The auto-induced uplink (a-UL) radio-frequency electromagnetic field (RF-EMF) exposure, often the dominant part of the total RF-EMF exposure, has not been included in previous microenvironmental studies. As 5G exposure depends more on mobile phone usage, monitoring typical transmit power levels is crucial towards more accurate personal exposure assessment. This study describes spatial differences in average mobile phone transmit power and investigates the influence of uplink duty cycles and frequency band usage. A novel methodology using the network monitoring application QualiPoc in fourth-generation (4G) and non-standalone fifth-generation (5G) networks was presented. For the first time, the assessment of 4G and 5G a-UL RF-EMF exposure was conducted simultaneously in a large-scale microenvironmental study in Europe. Measurements were performed along predefined routes in 282 different microenvironments (e.g., parks, residential areas) across seven European countries, during a maximum uplink usage scenario. The Netherlands had the highest average transmit powers per microenvironment (median 20.6 dBm). Transmit powers in villages were 0.6–2.1 dB higher than in big cities. The study suggested that base station density is a key predictor of a-UL exposure. Comparing technologies and frequency bands, average transmit powers for 5G were about 3.3 dB lower than for 4G and lowest for frequency bands with a time division duplexing (TDD) scheme due to the low uplink duty cycle (below 20%). This study provides crucial measurement data for epidemiologists and governments to enhance the understanding of the a-UL component of personal RF-EMF exposure.

* Corresponding author.
E-mail addresses: bram.stroobandt@ugent.be (B. Stroobandt), wout.joseph@ugent.be (W. Joseph).

https://doi.org/10.1016/j.envres.2025.121029
Received 5 November 2024; Received in revised form 16 January 2025; Accepted 2 February 2025
Available online 3 February 2025

1. Introduction

The deployment of the fifth-generation (5G) of mobile networks introduces new challenges for radio-frequency electromagnetic field (RF-EMF) exposure assessment compared to legacy technologies. The exposure depends much more on one's own mobile phone usage (Velghe et al., 2021). Additionally, dynamic capabilities of 5G lead to more spatio-temporal variability in RF-EMF exposure, primarily affecting the downlink (from the base station to the user). However, it also indirectly influences uplink exposure (from the user to the base station) through power control mechanisms that dynamically adjust the mobile phone's transmit power to maintain optimal signal quality, extend battery life, and improve overall network performance (Gati et al., 2010). Legacy technologies, such as the fourth-generation (4G) mobile networks, also exhibit these power control mechanisms but their RF-EMF exposure is less dependent on mobile phone usage because they have less dynamic (downlink) capabilities. The current non-standalone 5G deployment uses the existing 4G network infrastructure, utilizing both 4G and 5G signals to enhance speed and connectivity while relying on the 4G core network. Therefore, it is crucial to consider both 4G and 5G technologies, along with their spatial and temporal variability, for accurate RF-EMF exposure assessment.

Microenvironmental studies aim to characterize typical RF-EMF exposure in different microenvironments (e.g., parks or residential areas) towards personal exposure assessment. Previous microenvironmental studies have mainly assessed environmental exposure (Chikha et al., 2024; Joseph et al., 2010; Loizeau et al., 2023; Röösli et al., 2010; Sagar et al., 2016, 2018; Thielens et al., 2018; Velghe et al., 2019), i.e., the involuntary exposure from base stations or from nearby mobile phone users, known as environmental uplink (e-UL) exposure (Velghe et al., 2021). However, the auto-induced component of uplink RF-EMF exposure (i.e., exposure from one's own mobile phone usage) is often the dominant part of the total RF-EMF exposure and has not been considered in previous measurement studies (Chiaraviglio et al., 2024; Schilling et al., 2022; Van Wel et al., 2021). Therefore, an activity-based approach for microenvironmental studies was proposed, where different usage scenarios are performed to better understand the auto-induced uplink (a-UL) exposure (Velghe et al., 2021). Distinguishing a-UL from e-UL exposure requires monitoring the data transmission of the user's device during these scenarios, providing insights into the connection quality and the transmission patterns in 4G and 5G networks.

To monitor data transmission, two methods have been used: deducing network parameters (e.g., transmit powers and uplink transmission times) of all devices from the base station, which requires cooperation with the network operator (Joshi et al., 2017, 2020), or extracting them from a mobile phone using a commercial network monitoring application. The latter approach was used for 4G in various studies using different applications: Azenqos at outdoor small-cells (Mazloum et al., 2019), Nemo handy at indoor locations (Mazloum et al., 2021), and QualiPoc at outdoor locations (Schilling et al., 2022). Non-standalone 5G was investigated using QualiPoc at outdoor locations (Vermeeren et al., 2024), and XCAL solo, both indoors and outdoors (Jung et al., 2023). A recent review of 5G exposure assessment tools indicated the applicability of QualiPoc and similar network monitoring applications for human RF-EMF exposure studies and emphasized the research potential of measurements in combined 4G and 5G networks (Korkmaz et al., 2024).

As an alternative for monitoring the data transmission, RF-EMF measurement devices can be used near the mobile phone during data transmission. Either using a near-field probe (Iyare et al., 2021; Sârbu et al., 2019) or a dedicated device attached to the mobile phone, such as the Devin (Mazloum et al., 2023) or the Add-on sensor (Van Bladel et al.). These devices are not capable of distinguishing a-UL from e-UL exposure when placed near other mobile phones but they can indicate general uplink exposure trends.

It has been shown that mobile phones transmit on average at less than 1% of their maximum transmit power while using 4G data applications, emphasizing the need to assess time-averaged transmit power levels for RF-EMF exposure assessment rather than maximal values (Joshi et al., 2017). Other research suggests assessing the empirical maximum transmit power scaled by uplink duty cycles to estimate an upper bound on typical time-averaged transmit power (Aerts et al., 2019; Joseph et al., 2013). Uplink duty cycles, defined as the percentages of time a phone transmits, are necessary to obtain typical time-averaged transmit powers from network monitoring applications (Liu et al., 2024). Measurements of uplink duty cycles for 4G and 5G were taken at fixed locations near a single base station in a recent study (Vermeeren et al., 2024). However, large-scale research on typical uplink duty cycles across various usage scenarios is lacking, as well as a combined time-average transmit power of 4G and (non-standalone) 5G.

The main objectives of this work are to: (1) provide a novel methodology to assess the a-UL RF-EMF exposure from both 4G and 5G technologies; (2) demonstrate the applicability of this method during a maximum uplink usage scenario in different European countries; (3) compare spatial differences in average uplink transmit power in different microenvironments across seven countries; and (4) provide an exploratory data analysis of the influence of frequency band usage and uplink duty cycle on average transmit powers from 4G and 5G technologies.

2. Methods

2.1. Measurement configuration

Measurements were conducted from February to October 2023 in 282 microenvironments across seven European countries: Belgium, Switzerland, Hungary, the Netherlands, the United Kingdom, Italy, and Poland. Trained researchers walked for approximately 15 minutes along predefined routes, ranging from 1 to 1.5 km in length, in each microenvironment (Röösli et al., 2010). Traveling between microenvironments was done using public transport, which was considered as separate microenvironments. The researchers adhered to the measurement protocol presented in a recent study in Switzerland (Veludo et al., 2025).

2.1.1. Classification of microenvironments

In each country, five different study areas were defined, based on population density and degree of urbanization following the Eurostat manual (Dijkstra et al., 2021) and the corresponding interactive map of Copernicus ("GHSL visualisation", 2020): one big city (usually the capital, with more than 500 000 inhabitants), one secondary city (between 100 000 and 500 000 inhabitants), and three villages (less than 100 000 inhabitants). Within each study area, microenvironments were classified into three main types: outdoor areas, public places, and public transport. Outdoor areas included residential, business, industrial, and downtown areas. Public places comprised both indoor and outdoor locations frequented by young people, such as primary and secondary schools, universities, shopping malls, public parks, and train, bus, and metro stations. Residential areas and public parks were further subdivided into central, non-central, and outskirt areas. Traveling by train, tram, bus, and metro was classified as public transport. A summary of the number of microenvironments and samples is provided in Table SI-A.1 in Supplementary Information A (SI-A). Each microenvironment was identified by a its microenvironmental code (ME_code), based on the above classification.

2.1.2. Measurement devices

Researchers carried a backpack containing three measurement devices, following the protocol presented in a recent study (Veludo et al., 2025). We focused on measurements with the commercial network monitoring application QualiPoc by Rohde & Schwarz ("QualiPoc Android," 2023). QualiPoc collects many network parameters, such as data throughput, transmit power, and frequency band, directly from the phone's chipset. QualiPoc Android version 22 was installed on four different smartphones. Three smartphones, equipped with a Qualcomm chipset (SM8350 Snapdragon 888 5G), were used: a OnePlus 9 Pro in Belgium and the Netherlands, a Xiaomi MI 11 in Hungary, and another Xiaomi MI 11 in Poland. The fourth smartphone, a Samsung Galaxy S22+ with an Exynos (2200) chipset, was used in Switzerland, the United Kingdom, and Italy. In each country, a unique SIM-card with a 5G unlimited subscription from a major mobile network provider was used.

2.1.3. Usage scenario

Along the route in each microenvironment, a maximum uplink exposure scenario was performed, where the mobile phone repeatedly uploaded a 500 MB file to a File Transfer Protocol (FTP) server at Ghent University. The phone was not restricted to any specific frequency band or telecommunication technology, ensuring realistic frequency band usage. This scenario aimed to obtain the empirical maximum a-UL exposure, as described by literature (Aerts et al., 2019; Standard IEC 62232:2017, 2017), providing an upper bound on the typical time-averaged exposure. It is assumed that other mobile phone usage scenarios (e.g., voice calls, video streaming) result in lower effective time-averaged a-UL exposure than this maximum uplink scenario, due to lower uplink resource utilization. Their typical time-averaged transmit powers can be inferred from the empirical maximum by rescaling with experimentally defined uplink duty cycles (Vermeeren et al., 2024). This approach allows for the assessment of multiple usage scenarios necessary for personal exposure assessment without repeating measurements.

2.2. Data analysis

In addition to network parameters, metadata was collected during measurements, including the type of microenvironment, exact start and stop times, and additional notes by the researchers. This metadata was gathered through an application on the researcher's personal phones. It was cleaned both manually, based on the researchers' notes and Global Positioning System (GPS) data from QualiPoc, and automatically, using QualiPoc throughput or GPS data. This process resulted in the accurate number of samples for each microenvironmental measurement, as shown in Table SI-A.1.

Failure of the maximum uplink scenario was assumed if the total throughput (4G and 5G) remained below 350 kilobit per second (kbps) for at least 30 s without a connection to legacy networks (2G or 3G). These periods were excluded from the data, accounting for 15 % of the total measurement time. Microenvironments with at least 60 s of data were included in the analysis. Table SI-A.1 provides the number of removed ("Fail") and retained ("Tot") samples per microenvironment for each country.

The QualiPoc data was extracted using ROMES software (by Rohde & Schwartz) ("ROMES Drive Test Software," 2024) and processed with Python. Table SI-A.2 lists the different network parameters obtained from QualiPoc. This study utilized Physical Uplink Shared Channel (PUSCH) transmit power, PUSCH throughput, transport block size, and frequency band parameters. For data cleaning2.2, Physical Downlink Shared Channel (PDSCH) throughput, Radio Resource Control (RRC) states, GPS coordinates, Global System for Mobile Communications (GSM) mode and Universal Mobile Telecommunications System (UMTS) transmit power were used.

The network parameters from QualiPoc (Table SI-A.2) are provided by the chipset of the mobile phone without a fixed sampling time. E.g., the frequency band parameter is immediately reported once it has changed. However, the transmit power, throughput, and transport block size parameters are provided approximately every 500 ms. They were only considered if the frequency band remained the same during the 500 ms period, to avoid over- or underestimation of the average transmit power during handovers (i.e., a switch to a different frequency band) within the same technology. It was chosen to use average samples per second for the network parameters, such that enough samples for each microenvironment could be obtained at a fixed granularity.

2.2.1. Average uplink transmit power per second

The average uplink transmit power per second P_{avg} was computed as the average of the 4G and 5G PUSCH transmit power (Table SI-A.2) using Equation (1). PUSCH was used to assess the a-UL exposure from uplink data usage only, excluding other signals such as network control.

$$P_{avg}[W] = DC_{4G}[-] \bullet P_{PUSCH,4G}[W] + DC_{5G}[-] \bullet P_{PUSCH,5G}[W] \tag{1}$$

$P_{PUSCH,xG}$ is the PUSCH transmit power of the specified technology averaged over 1 s. DC_{xG} is the uplink duty cycle for the specified network technology, defined as the average ratio of active uplink slots to the total number of slots in the considered 1-s intervals. Its calculation is explained in detail in Supplementary Information B (SI-B).

Multiplying $P_{PUSCH,xG}$ by the uplink duty cycle was necessary because the reported PUSCH transmit power is an average over approximately 500 ms, including only values that are reported by the chipset. This differs from instantaneous power measurements with a predefined sampling time. Using $P_{PUSCH,xG}$ directly in the analysis could significantly overestimate exposure, as it would extrapolate the active uplink slots (i.e., the uplink slots used to transmit data at the reported power) to all available slots within the 1-s interval. By multiplying $P_{PUSCH,xG}$ by the uplink duty cycle, slots with no transmission are also considered, providing the true average transmit power. Finally, P_{avg} [W] was converted to [dBm] for analysis in Section 3.

2.2.2. Average uplink transmit power per microenvironment

The arithmetic mean $P_{avg,ME}$ of the P_{avg} values (after data cleaning) along the microenvironmental routes was computed using Equation (2):

$$P_{avg,ME}\ [W] = \frac{1}{N}\sum_{n} P_{avg}\ [W] \tag{2}$$

where N is the number of samples (equal to the number of seconds), as shown in Table SI-A.1, and P_{avg} is the PUSCH transmit power averaged over 1 s, as defined by Equation (1).

If multiple microenvironments of the same type were measured within the same country, e.g., public transport, they were merged and $P_{avg,ME}$ was computed over all samples. This is indicated by the number of microenvironments in Table SI-A.1.

2.2.3. Average uplink duty cycle per microenvironment

Analogous to the computation of $P_{avg,ME}$, the arithmetic mean of DC_{xG} along the route (after data cleaning) was computed using Equation (3) to provide insight into the differences between 4G and 5G technologies in terms of uplink duty cycles.

$$DC_{xG,avg,ME}[-] = \frac{1}{N}\sum_{n} DC_{xG}[-] \tag{3}$$

2.2.4. Stratification per frequency band

From QualiPoc, the frequency bands used for the connection between the mobile phone and the base station were extracted. This enabled the assessment of differences in transmit power across various frequency bands. For each microenvironment, the transmit power, throughput, and transport block size parameter values were stratified per frequency band to apply the band-specific subcarrier spacing in the calculation of the uplink duty cycle. Subsequently, P_{avg} was computed, including the frequency band in use for both 4G and 5G.

For clarity, uplink carrier aggregation (CA) or uplink control signals in the physical uplink control channel (PUCCH) were not investigated. Their influence was expected to be small, as little CA was observed across the countries and control signals are often multiplexed on the PUSCH (Dahlman et al., 2018, pp. 221–223). The study was limited to 4G and 5G due to significant differences between technologies, such as the absence of PUSCH in the 3G network protocol.

3. Results and discussion

3.1. Spatial comparison of the average transmit power per microenvironment

We performed a descriptive statistical analysis of $P_{avg,ME}$, comparing countries, cities and villages, and microenvironments. The values of $P_{avg,ME}$ are provided in Table SI-A.3.

3.1.1. Comparison of average transmit power between countries

Fig. 1 shows boxplots of $P_{avg,ME}$ for the different countries, including both 4G and 5G transmit powers following Equations (1) and (2). Values of $P_{avg,ME}$ between 1.6 dBm and 23.6 dBm were found, except for 1 outlier in Poland. The distributions were negatively skewed and their median and inter-quartile range (IQR) were listed in Table 1. The highest median $P_{avg,ME}$ was 20.6 dBm and was found in the Netherlands, followed by Belgium (19.8 dBm), Hungary (19.6 dBm), and Italy (19.2 dBm). The medians in Switzerland (17.7 dBm) and Poland (17.0 dBm) were about 2 dB lower. The lowest median $P_{avg,ME}$ was 13.2 dBm and was found in the United Kingdom.

The maximum uplink usage scenario demands for a good uplink connection at any location, which leads to high values of $P_{avg,ME}$ in general. The highest values of $P_{avg,ME}$ (indicated by the top whiskers in Fig. 1) were below the maximum transmit power of 23 dBm, except for the Netherlands. However, 23.6 dBm remained within the +2/-3 dB tolerance level defined in the technology specification (5G NR, 2021). The lower median in Switzerland and Poland can be attributed to better network connections. Switzerland hosted Europe's first commercial 5G network and thus is ahead of other countries with its 5G deployment. In Poland, more strict exposure limits require a higher base station density (Pawlak et al., 2019). The distribution of $P_{avg,ME}$ in the United Kingdom extended to much lower values due to missing 4G samples in the QualiPoc data, which caused $P_{avg,ME}$ to include 5G only while both 4G and 5G were used simultaneously.

3.1.2. Comparison of average transmit power between cities and villages

Fig. 2 shows the distributions of $P_{avg,ME}$ stratified in big cities, secondary cities, and villages for the different countries. Villages exhibited the highest median $P_{avg,ME}$ compared to the cities in Belgium, the Netherlands, Hungary, and Switzerland. In Italy, the United Kingdom, and Poland, the secondary city had the highest median $P_{avg,ME}$. The median of the big cities was between 0.6 dB (in Italy) and 2.1 dB (in the Netherlands) lower than the median of the villages.

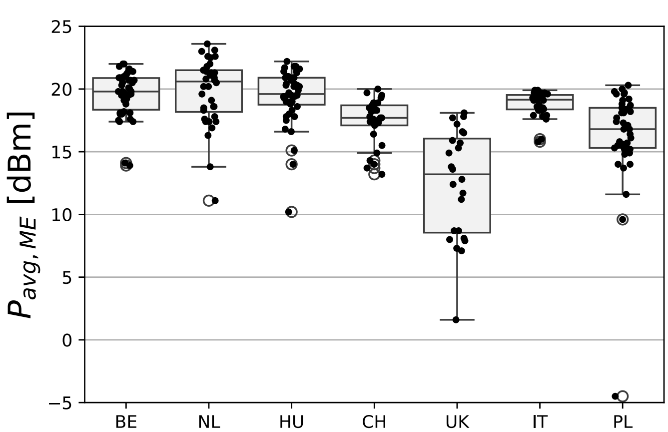

Fig. 1. Boxplots of $P_{avg,ME}$ for each country (x-axis); BE = Belgium, NL = the Netherlands, HU = Hungary, CH = Switzerland, UK = the United Kingdom, IT = Italy, PL = Poland. The whiskers represent the lowest and highest data points (black dots) that are found within 1.5 IQR difference from the median (middle horizontal black line). All other samples are represented as outliers (black circles).

Table 1
Summary statistics of $P_{avg,ME}$ [dBm] per country.

Statistic [unit]	BE[a]	NL[a]	HU[a]	CH[a]	UK[a]	IT[a]	PL[a]
Median [dBm]	19.8	20.6	19.6	17.7	13.2	19.2	17.0
IQR [dB]	2.5	3.3	2.2	1.6	7.5	1.2	3.2

[a] Country abbreviations; BE = Belgium, NL = the Netherlands, HU = Hungary, CH = Switzerland, UK = United Kingdom, IT = Italy, PL = Poland.

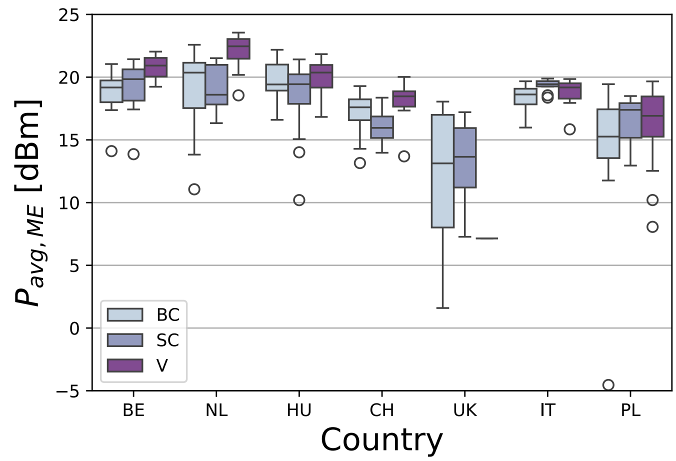

Fig. 2. Boxplots of $P_{avg,ME}$ per study area in each country (x-axis); BE = Belgium, NL = the Netherlands, HU = Hungary, CH = Switzerland, UK = United Kingdom, IT = Italy, PL = Poland. The whiskers represent the lowest and highest data points that are found within 1.5 IQR difference from the median (black line). All other samples are represented as outliers (circles). BC = Big City, SC = Secondary City, V = Villages.

The highest uplink transmit powers generally found in villages can be attributed to a lower base station density, which confirms the results for 4G transmit powers found in a previous study (Joshi et al., 2017). In both Italy and Poland, one of the three villages had significantly lower values compared to the other two. This is explained by the presence of a base station in the center of these villages, which indicates that proximity to a base station can result in lower transmit powers compared to similar areas with a low base station density. The low value for the villages in the United Kingdom (7.15 dBm) was not considered in the analysis due to the exclusive availability of bus ride data. All other microenvironments in these villages were excluded because only 3G was used, which could not be investigated. The difference in median $P_{avg,ME}$ between big cities and villages was 1.2 dB – 2.7 dB smaller than the 3.3 dB difference observed for 4G transmit powers between urban and rural areas reported in the previous study (Joshi et al., 2017). This was anticipated due to the maximum uplink usage scenario, which generally leads to higher uplink transmissions, and the use of non-standalone 5G networks.

3.1.3. Comparison of average transmit power between individual microenvironments

Table 2 presents the microenvironments with the highest and lowest values of $P_{avg,ME}$ in each country, along with their corresponding values. The majority of microenvironments with the highest $P_{avg,ME}$ were located in outskirt parks or various village microenvironments. In the United Kingdom, the highest $P_{avg,ME}$ value was recorded during a bus ride. In Poland, the highest value was found in the non-central residential area of the big city. Conversely, the lowest average uplink transmit powers were mainly observed in big cities or industrial areas, with one instance in a primary school of a secondary city.

Villages and outskirt parks are locations where larger distances to the

Table 2
Maximal (Max.) and minimal (Min.) values of $P_{avg,ME}$ for each country and the corresponding microenvironment, identified by its ME_code[a].

Country	Max. [dBm]	Max. microenvironment	Min. [dBm]	Min. microenvironment
Belgium	22.0	V2_OA_center	13.9	SC_PP_primaryschool
Netherlands	23.6	V2_PP_park	11.1	BC_PP_trainstation
Hungary	22.2	BC_PP_park_OUT	10.2	SC_OA_industrial
Switzerland	20.0	V3_PP_park	13.2	BC_OA_residential_C
UK	18.1	BC_PT_busride	1.6	BC_PT_trainride
Italy	19.9	SC_PP_park_OUT	15.8	V1_OA_industrial
Poland	20.3	BC_OA_residential_NC	−4.5	BC_OA_business

[a] ME_code abbreviations; BC = big city, SC = secondary city, V = village, OA = outdoor area, PP = public place, PT = public transport, C = central, NC = non-central, OUT = outskirts.

nearest base stations are expected, leading to higher uplink transmit powers (thus higher $P_{avg,ME}$) due to the power control mechanism. In contrast, big cities and industrial areas are expected to have higher base station densities. The low $P_{avg,ME}$ observed in the primary school is attributed to the presence of a base station across the street. These findings suggested that base station density is one of the main predictors of a-UL exposure. This aligns with the higher 4G transmit powers in rural areas found in a previous study which was attributed to greater distances between base stations and mobile phones (Joshi et al., 2017). However, base station density does not account for all the variability in $P_{avg,ME}$ values found across different microenvironments within each country.

The distributions of the average transmit power per second (P_{avg}) for all individual microenvironments in each country are depicted in Figures SI-A.1-7. Based on the principles discussed earlier, we anticipated that P_{avg} values would be higher in outskirt areas and lower in central city areas. However, we observed no consistent trend across countries. Additionally, the distributions of P_{avg} varied significantly between microenvironments of the same type, indicating that differences are not solely explained by the spatial properties of the microenvironment. Other methods, such as clustering techniques or other machine learning-based classification algorithms, are required to explain this intraclass variability. The numerous amount of parameters available from the QualiPoc network monitoring software can provide new features to be utilized in these machine learning models.

3.2. 4G and 5G average uplink duty cycles

Fig. 3 shows the distributions of the uplink duty cycles $DC_{4G,avg,ME}$ and $DC_{5G,avg,ME}$, as defined by Equation (3), for each country. The values

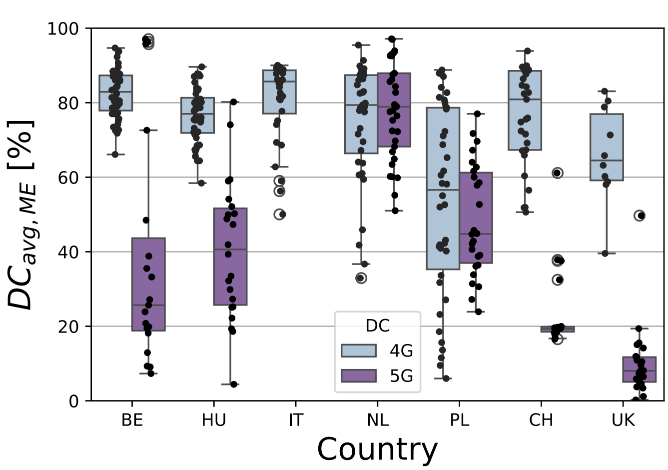

Fig. 3. Boxplots of $DC_{4G,avg,ME}$ and $DC_{5G,avg,ME}$ per country; BE = Belgium, NL = the Netherlands, HU = Hungary, CH = Switzerland, UK = United Kingdom, IT = Italy, and PL = Poland. DC = uplink duty cycle.

for each microenvironment are detailed in Table SI-A.4. In all countries, the median of $DC_{4G,avg,ME}$ exceeded the median of $DC_{5G,avg,ME}$ by 12–62 percentage point, except in the Netherlands and Italy. The difference in median was negligible in the Netherlands, and no 5G was observed in Italy. For most countries, the values of $DC_{4G,avg,ME}$ were greater than 77 %, except for the UK and Poland.

P_{avg} is influenced by the uplink duty cycles. The higher 4G and lower 5G uplink duty cycles in most countries indicate that 4G is still the primary contributor to a-UL exposure. We expect a shift towards 5G in the coming years. The similar mean values in the Netherlands are attributed to differences in frequency band usage, which is examined in Section 3.4.

3.3. Frequency bands

Table 3 lists the eleven different frequency bands observed during the maximum uplink scenario across all seven European countries and their corresponding frequency ranges. Three of these ranges were used for both 4G and 5G technologies. All but band n78 (3500 MHz) and band 40 (2300 MHz) were frequency division duplexing (FDD) bands, which means that the frequency range was configured for uplink signals only and a separate frequency range for downlink signals was located at slightly higher frequencies. The TDD bands, on the other hand, were configured for both uplink and downlink signals using short time slots with a fixed length. The 4G bands 20, 3, and 7 (800 MHz, 1700 MHz, and 2500 MHz; Table 3) were the only bands used for uplink transmission at least once in each of the countries.

3.4. Transmit power and uplink duty cycle per frequency band

Fig. 4 shows the average transmit power per microenvironment $P_{avg,ME,band\ i}$ (a) and the average uplink duty cycle per microenvironment $DC_{avg,ME,band\ i}$ (b), stratified per frequency band. The highest values of $P_{avg,ME,band\ i}$ were found for 4G band 28 (700 MHz), with a median of 21.0 dBm. The distributions of $P_{avg,ME,band\ i}$ and $DC_{avg,ME,band\ i}$ of the other 4G FDD bands had similar ranges, excluding outliers, between 11.1 dBm and 22.4 dBm and between 40 % and 100 %, respectively. The 4G TDD band 40 (2300 MHz), was present for 1 microenvironment with $P_{avg,ME,band\ i}$ equal to 11.9 dBm. All medians of $P_{avg,ME,band\ i}$ were below 17.5 dBm for frequency bands above 1.9 GHz. For frequency bands below 1.9 GHz, the medians were above 17.5 dBm, except for 5G Band n3 (17.4 dBm).

The transmit powers over 5G bands n1 and n3, operating at legacy frequency ranges, had medians of 16.3 dBm and 17.4 dBm, respectively. This was between 1.1 dB (band n1, 1900 MHz) and 1.2 dB (band n3, 1800 MHz) lower than the medians for the same frequency ranges used for 4G (i.e., bands 1 and 3). They had similar ranges of $DC_{avg,ME,band\ i}$, except for the n1-band in Poland, where the $DC_{avg,ME,band\ i}$ was much lower (not distinguished in Fig. 4b) with values below 70 % in 23 out of 25 microenvironments compared to 1 out of 7 microenvironments in Hungary and 2 out of 15 microenvironments in Belgium.

Table 3
Frequency band ranges and their names with corresponding technology and duplexing scheme. FDD = frequency division duplexing, TDD = time division duplexing.

Technology, band, and duplex scheme	Frequency range [MHz]
4G Band 28 (FDD), 5G Band n28 (FDD)	703–748
4G Band 20 (FDD)	832–862
4G Band 8 (FDD)	880–915
4G Band 3 (FDD), 5G Band n3 (FDD)	1710–1785
4G Band 1 (FDD), 5G Band n1 (FDD)	1920–1980
4G Band 40 (TDD)	2300–2400
4G Band 7 (FDD)	2500–2570
5G Band n78 (TDD)	3300–3800

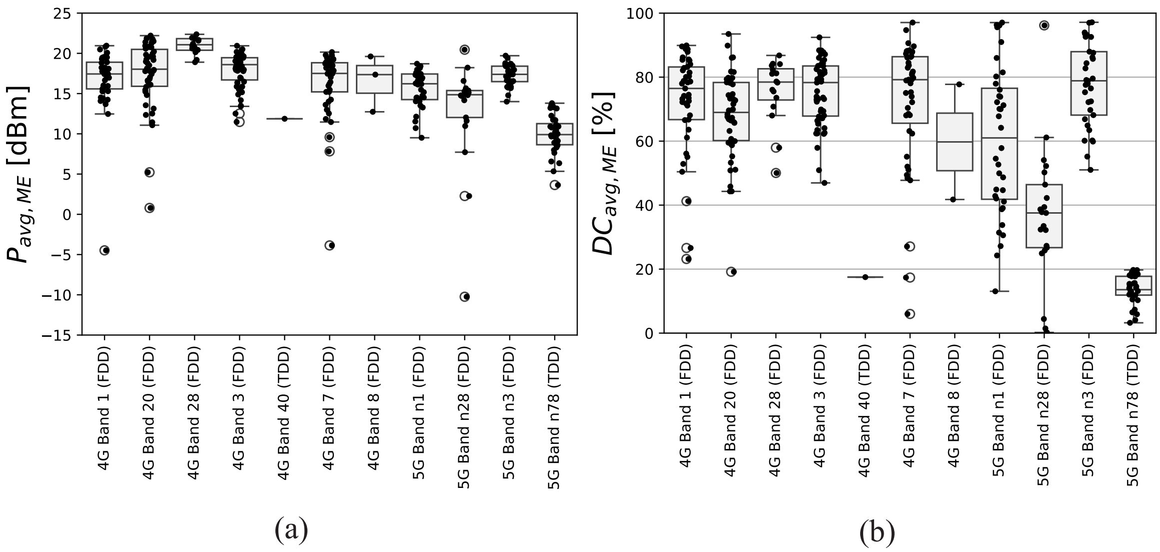

Fig. 4. $P_{avg,ME,band\ i}$ (a) and $DC_{avg,ME,band\ i}$ (b) per frequency band i (x-axis) across all European countries.

The median of $P_{avg,ME,band\ i}$ for the 5G TDD band n78 (3500 MHz) was 3 dB lower than the median for 5G FDD band n28 (700 MHz), both recently introduced frequency bands. Their median $DC_{avg,ME,band\ i}$ values were below 61 % (TDD band n78, 3500 MHz) and 20 % (FDD band n28, 700 MHz), respectively. The uplink duty cycle for both 4G and 5G TDD bands (band 40 and n78) remained below 20 %. The average transmit power for 5G bands was generally lower than for 4G bands, by approximately 3.3 dB.

The current non-standalone 5G implementation implies that most signals are still sent over the 4G network, with 5G used for larger bandwidth where 5G base stations are present. The 4G bands serve as the anchor frequencies of the core network and 5G is used simultaneously as an additional resource (Agiwal et al., 2021).

The 4G band 28 (700 MHz) has the lowest frequency range observed (see Table 3) and the highest median $P_{avg,ME}$. Low frequency bands provide larger coverage, so the mobile phone is likely to connect to and send uplink data at lower frequencies when near the cell edge (i.e., far from the base station). The large distance requires high transmit powers to reach the base station. This is true when considering the usage of one technology and one frequency band at the same time. The flexibility in uplink resource allocation and instantaneous transmit power, as well as the use of multiple 4G or 5G cells and frequency bands, complicates the analysis. A trade-off is made between fast transmission (high uplink duty cycle) and high instantaneous transmit powers, while staying below the transmit power limit of 23 dBm (+2/-3 dB tolerance). Further investigation is needed to analyze this behavior for different frequency band combinations.

Legacy FDD frequency bands have similar uplink duty cycles for both technologies but lower $P_{avg,ME,band\ i}$ for 5G than 4G, since 5G is used only when closer to the base station and always on top of 4G. In Poland, lower uplink duty cycle values for band n1 indicate that 5G is used less than 4G, possibly due to stricter exposure limits.

The difference in uplink duty cycle and transmit power between recently introduced 5G frequency bands n78 (3500 MHz) and n28 (700 MHz) may be attributed to the TDD scheme compared to the FDD scheme. The maximal uplink duty cycle for TDD is equal to 23 % as recommended by these guidelines (5G TDD, 2020). This explains why $P_{avg,ME,band\ i}$ in Fig. 4a does not exceed 16.6 dBm for both TDD bands, considering the transmit power limit of 23 dBm.

The uplink duty cycle values of Fig. 4b are about 22 and 7 percentage point lower for 4G (93 %) and 5G (20 %), respectively, than uplink duty cycles measured in a recent study for fixed locations near a base station in Belgium (Vermeeren et al., 2024). The study observed less variability in the uplink duty cycle during a similar FTP upload with a larger file size (10 GB), which highlights the importance of capturing the variability within microenvironments for realistic a-UL exposure assessment.

$P_{avg,ME,band\ i}$ and $DC_{avg,ME,band\ i}$ per frequency band are provided in Table SI-A.6.

3.5. Strengths and limitations

We used the network monitoring application QualiPoc in a microenvironmental study for the first time. This enabled the collection of a numerous amount of network parameters in real mobile networks, useful for realistic RF-EMF exposure assessment. Frequency band usage gathered from QualiPoc enabled the stratification of 4G and 5G transmit powers and uplink duty cycles per frequency band. The multiplication of the PUSCH transmit power values with the uplink duty cycle for every frequency band separately, made sure that typical average exposure values were obtained for which the TDD factor is included. Since the monitoring app gathered data from the chipset of the mobile phone only, the a-UL exposure was automatically distinguished from the e-UL exposure as opposed to the use of frequency-selective exposure meters. A well-designed measurement protocol (Veludo et al., 2025) ensured the similar operation of trained researchers in various countries, enhancing the reliability of the measurement data. This study paved the way forward to personal exposure assessment of European citizens, providing crucial measurement data for epidemiologists and governments to enhance the understanding of typical a-UL exposure.

However, the amount of microenvironments where we gathered useful measurement data was limited for some study areas and the repeatability of these measurements was not investigated. Additionally, the readings from QualiPoc were completely dependent on the phone's chipset, over which the researcher has no control. The study was limited to 4G and 5G technologies. Although these are the most used technologies in most of the considered European countries, this limited the analysis of the rural areas in the United Kingdom where a lot of 3G was still used. The measurements were subject to the network behavior at the time of measurement, which is a crucial limitation. The influence of other users and network-specific settings on throughput variability, connection loss, and the use of specific technologies or frequency bands was unclear. Moreover, only one of the main network operators was represented in each country. Although a study of 5G transmit powers reported no significant differences between three different operators in the city of Seoul, South-Korea (Lee et al., 2021), different operators might make use of different frequency bands, duty cycles, 5G deployment, and network priorities across the many European microenvironments investigated in this study which limits the generalization of the results towards different network operators.

4. Conclusions

This study introduced a novel methodology to measure the auto-induced uplink (a-UL) radio-frequency electromagnetic field (RF-EMF) exposure from a mobile, including non-standalone 5G for the first time in a large-scale European microenvironmental study. Average transmit power and uplink duty cycles of the mobile phone were investigated across different microenvironments in Europe as well as their relation to the frequency band usage. Measurements in 282 different microenvironments across seven European countries showed that the highest average uplink transmit powers (median 20.6 dBm) were found in the Netherlands, with villages generally having 0.6–2.1 dB higher transmit powers than big cities. The study suggested that base station density is a key predictor of a-UL exposure and found that transmit powers for 5G were generally about 3.3 dB lower than for 4G. Future research will assess measurements repeated after two years to track changes in the 5G technology and its influence on a-UL RF-EMF exposure.

CRediT authorship contribution statement

Bram Stroobandt: Writing – review & editing, Writing – original draft, Visualization, Software, Methodology, Investigation, Formal analysis, Data curation. **Han Van Bladel:** Writing – review & editing, Formal analysis, Data curation. **Adriana Fernandes Veludo:** Writing – review & editing, Formal analysis, Data curation. **Kenneth Deprez:** Writing – review & editing, Software. **Sam Aerts:** Writing – review & editing, Methodology. **Leen Verloock:** Writing – review & editing. **György Thuróczy:** Writing – review & editing. **Piotr Politanski:** Writing – review & editing. **Kinga Polanska:** Writing – review & editing, Funding acquisition, Conceptualization. **Gabriella Tognola:** Writing – review & editing, Funding acquisition, Conceptualization. **Marta Parazzini:** Writing – review & editing, Funding acquisition, Conceptualization. **Joe Wiart:** Writing – review & editing, Funding acquisition, Conceptualization. **Mònica Guxens:** Writing – review & editing, Funding acquisition, Conceptualization. **Martin Röösli:** Writing – review & editing, Funding acquisition, Conceptualization. **Wout Joseph:** Writing – review & editing, Supervision, Funding acquisition, Formal analysis, Conceptualization.

Declaration of the use of AI in the scientific writing process

During the preparation of this work the authors used Bing Copilot in order to filter out non-essential parts and to improve the readability of the manuscript. After using this tool, the authors reviewed and edited the content as needed and take full responsibility for the content of the published article.

Ethical considerations

The study did not involve humans as subjects and did not collect any personal and/or health data. Thus, no ethical approval is needed according to the laws of the participating countries.

Data statement

The code to reproduce the analysis will be made available via the open repository 'dataverse' of the Consorci de Serveis Universitaris de Catalunya (CSUC). The datasets generated and analysed in this study can be made available upon request to the last author, Wout Joseph (wout.joseph@ugent.be).

Funding

This project has received funding from the European Union's Horizon Europe research and innovation programme under grant agreement No 101057262. Views and opinions expressed are however those of the authors only and do not necessarily reflect those of the European Union or the Health and Digital Executive Agency. Neither the European Union nor the granting authority can be held responsible for them. We acknowledge support from the grant CEX2023-0001290-S funded by MCIN/AEI/10.13039/501100011033, and support from the Generalitat de Catalunya through the CERCA Program. Mònica Guxens was funded by a Miguel Servet II fellowship (CPII18/00018) awarded by the Spanish Institute of Health Carlos III.

Declaration of competing interest

The authors declare that they have no known competing financial interests or personal relationships that could have appeared to influence the work reported in this paper.

Acknowledgements

The authors greatly acknowledge all people involved in the data collection process, apart from themselves, namely: Ms. Lea Beláccková from Utrecht University (the Netherlands), Dr. Zsuzsanna Vecsei from the National Center for Public Health and Pharmacy (Hungary), and Dr. Marta Bonato, Dr. Silvia Gallucci, and Dr. Martina Benini from CNR (Italy).

Appendix A. Supplementary data

Supplementary data to this article can be found online at https://doi.org/10.1016/j.envres.2025.121029.

Data availability

Data will be made available on request. The code to reproduce the analysis will be made available via the open repository 'dataverse' of the Consorci de Serveis Universitaris de Catalunya (CSUC). The datasets generated and analysed in this study can be made available upon request to the last author, Wout Joseph (https://wout.joseph@ugent.be).

References

5G NR, 2021. User Equipment (UE) radio transmission and reception; Part 3: range 1 and Range 2 Interworking operation with other radios. https://www.etsi.org/deliver/etsi_ts/138100_138199/13810103/15.03.00_60/ts_13810103v150300p.pdf (Accessed 29 August 2024).

5G TDD, 2020. Synchronisation guidelines and Recommendations for the coexistence of TDD networks in the 3. 5 GHz Range. https://www.gsma.com/connectivity-for-good/spectrum/wp-content/uploads/2020/04/3.5-GHz-5G-TDD-Synchronisation.pdf (Accessed 29 August 2024).

Aerts, S., Verloock, L., Van Den Bossche, M., Colombi, D., Martens, L., Törnevik, C., Joseph, W., 2019. In-situ measurement methodology for the assessment of 5G NR massive MIMO base station exposure at sub-6 GHz frequencies. IEEE Access 7, 184658–184667. https://doi.org/10.1109/ACCESS.2019.2961225.

Agiwal, M., Kwon, H., Park, S., Jin, H., 2021. A survey on 4G-5G dual connectivity: road to 5G implementation. IEEE Access 9, 16193–16210. https://doi.org/10.1109/ACCESS.2021.3052462.

Chiaraviglio, L., Lodovisi, C., Bartoletti, S., Elzanaty, A., Slim-Alouini, M., 2024. Dominance of smartphone exposure in 5G mobile networks. IEEE Trans. Mobile Comput. 23, 2284–2302. https://doi.org/10.1109/TMC.2023.3252662.

Chikha, W.B., Zhang, Y., Liu, J., Wang, S., Sandeep, S., Guxens, M., Veludo, A.F., Röösli, M., Joseph, W., Wiart, J., 2024. Assessment of radio frequency electromagnetic field exposure induced by base stations in several micro-environments in France. IEEE Access 12, 21610–21620. https://doi.org/10.1109/ACCESS.2024.3363914.

Dahlman, E., Parkvall, S., Skold, J., 2018. 5G NR: the Next Generation Wireless Access Technology, first ed. Academic Press, San Diego, CA.

Dijkstra, L., Brandmüller, T., Kemper, T., Asfandiyar, A., Veneri, P., 2021. Applying the Degree of Urbanisation — a methodological manual to define cities, towns and rural areas for international comparisons. https://ec.europa.eu/eurostat/statistics-explai

ned/index.php?title=Applying_the_degree_of_urbanisation_manual. (Accessed 7 January 2025).
Gati, A., Conil, E., Wong, M.-F., Wiart, J., 2010. Duality between uplink local and downlink whole-body exposures in operating networks. IEEE Trans. Electromagn C. 52, 829–836. https://doi.org/10.1109/TEMC.2010.2066978.
Global Human Settlement Layer Visualisation - European Commission, 2020. https://human-settlement.emergency.copernicus.eu/visualisation.php#. (Accessed 7 January 2025).
Iyare, R.N., Volskiy, V., Vandenbosch, G.A.E., 2021. Comparison of peak electromagnetic exposures from mobile phones operational in either data mode or voice mode. Environ. Res. 197, 110902. https://doi.org/10.1016/j.envres.2021.110902.
Joseph, W., Frei, P., Roösli, M., Thuróczy, G., Gajsek, P., Trcek, T., Bolte, J., Vermeeren, G., Mohler, E., Juhász, P., Finta, V., Martens, L., 2010. Comparison of personal radio frequency electromagnetic field exposure in different urban areas across Europe. Environ. Res. 110, 658–663. https://doi.org/10.1016/j.envres.2010.06.009.
Joseph, W., Pareit, D., Vermeeren, G., Naudts, D., Verloock, L., Martens, L., Moerman, I., 2013. Determination of the duty cycle of WLAN for realistic radio frequency electromagnetic field exposure assessment. Prog. Biophys. Mol. Biol. 111, 30–36. https://doi.org/10.1016/j.pbiomolbio.2012.10.002.
Joshi, P., Colombi, D., Thors, B., Larsson, L.-E., Tornevik, C., 2017. Output power levels of 4G user equipment and implications on realistic RF EMF exposure assessments. IEEE Access 5, 4545–4550. https://doi.org/10.1109/ACCESS.2017.2682422.
Joshi, P., Ghasemifard, F., Colombi, D., Tornevik, C., 2020. Actual output power levels of user equipment in 5G commercial networks and implications on realistic RF EMF exposure assessment. IEEE Access 8, 204068–204075. https://doi.org/10.1109/ACCESS.2020.3036977.
Jung, J., Lee, S., Shin, J., Kim, Y., 2023. Self-attention-based uplink radio resource prediction in 5G dual connectivity. IEEE Internet Things J. 10, 19925–19936. https://doi.org/10.1109/JIOT.2023.3283490.
Korkmaz, E., Aerts, S., Coesoij, R., Bhatt, C.R., Velghe, M., Colussi, L., Land, D., Petroulakis, N., Spirito, M., Bolte, J., 2024. A comprehensive review of 5G NR RF-EMF exposure assessment technologies: fundamentals, advancements, challenges, niches, and implications. Environ. Res. 260, 119524. https://doi.org/10.1016/j.envres.2024.119524.
Lee, A.-K., Jeon, S.-B., Choi, H.-D., 2021. EMF levels in 5G new radio environment in Seoul, Korea. IEEE Access 9, 19716–19722. https://doi.org/10.1109/ACCESS.2021.3054363.
Liu, J., Zhang, Y., Chikha, W.B., Wang, S., Samaras, T., Jawad, O., Ourak, L., Conil, E., Wiart, J., 2024. Assessment of EMF exposure induced by wireless cellular phones in various usage scenarios in France. IEEE Access. https://doi.org/10.1109/ACCESS.2024.3424305, 1–1.
Loizeau, N., Zahner, M., Schindler, J., Stephan, C., Fröhlich, J., Gugler, M., Ziegler, T., Röösli, M., 2023. Comparison of ambient radiofrequency electromagnetic field (RF-EMF) levels in outdoor areas and public transport in Switzerland in 2014 and 2021. Environ. Res. 237, 116921. https://doi.org/10.1016/j.envres.2023.116921.
Mazloum, T., Aerts, S., Joseph, W., Wiart, J., 2019. RF-EMF exposure induced by mobile phones operating in LTE small cells in two different urban cities. Ann. Telecommun. 74, 35–42. https://doi.org/10.1007/s12243-018-0680-1.
Mazloum, T., Wang, S., Hamdi, M., Ashenafi Mulugeta, B., Wiart, J., 2021. Artificial neural network-based uplink power prediction from multi-floor indoor measurement campaigns in 4G networks. Front. Public Health 9. https://doi.org/10.3389/fpubh.2021.777798.
Mazloum, T., Bories, S., Dassonville, D., Wiart, J., 2023. Impact of sampling frequency on the performance of DEVIN: a personal EM UL exposimeter. In: 2023 XXXVth General Assembly and Scientific Symposium of the International Union of Radio Science (URSI GASS). Presented at the 2023 XXXVth General Assembly and Scientific Symposium of the International Union of Radio Science (URSI GASS), pp. 1–4. https://doi.org/10.23919/URSIGASS57860.2023.10265631.
Pawlak, R., Krawiec, P., Żurek, J., 2019. On measuring electromagnetic fields in 5G technology. IEEE Access 7, 29826–29835. https://doi.org/10.1109/ACCESS.2019.2902481.
QualiPoc, 2023. Android. https://www.rohde-schwarz.com/us/products/test-and-measurement/network-data-collection/qualipoc-android_63493-55430.html. (Accessed 21 October 2024).
ROMES, 2024. Drive test software. https://www.rohde-schwarz.com/us/brochure-datasheet/romes/. (Accessed 29 August 2024).
Röösli, M., Frei, P., Bolte, J., Neubauer, G., Cardis, E., Feychting, M., Gajsek, P., Heinrich, S., Joseph, W., Mann, S., Martens, L., Mohler, E., Parslow, R.C., Poulsen, A. H., Radon, K., Schüz, J., Thuroczy, G., Viel, J.-F., Vrijheid, M., 2010. Conduct of a personal radiofrequency electromagnetic field measurement study: proposed study protocol. Environ. Health 9, 23. https://doi.org/10.1186/1476-069X-9-23.
Sagar, S., Struchen, B., Finta, V., Eeftens, M., Röösli, M., 2016. Use of portable exposimeters to monitor radiofrequency electromagnetic field exposure in the everyday environment. Environ. Res. 150, 289–298. https://doi.org/10.1016/j.envres.2016.06.020.
Sagar, S., Adem, S.M., Struchen, B., Loughran, S.P., Brunjes, M.E., Arangua, L., Dalvie, M. A., Croft, R.J., Jerrett, M., Moskowitz, J.M., Kuo, T., Röösli, M., 2018. Comparison of radiofrequency electromagnetic field exposure levels in different everyday microenvironments in an international context. Environ. Int. 114, 297–306. https://doi.org/10.1016/j.envint.2018.02.036.
Sârbu, A., Bechet, A., Bălan, T., Robu, D., Bechet, P., Miclăuş, S., 2019. Using CCDF statistics for characterizing the radiated power dynamics in the near field of a mobile phone operating in 3G+ and 4G+ communication standards. Measurement 134, 874–887. https://doi.org/10.1016/j.measurement.2018.12.018.
Schilling, L.-M., Bornkessel, C., Hein, M.A., 2022. Impact of small-cell deployment on combined uplink and downlink RF exposure compared to the status quo in mobile networks. In: 2021 51st European Microwave Conference (EuMC). Presented at the 2021 51st European Microwave Conference (EuMC). IEEE, London, United Kingdom, pp. 618–621. https://doi.org/10.23919/EuMC50147.2022.9784284.
Standard IEC 62232:2017, 2017. Determination of RF Field Strength, Power Density and SAR in the Vicinity of Radiocommunication Base Stations for the Purpose of Evaluating Human Exposure.
Thielens, A., Van den Bossche, M., Brzozek, C., Bhatt, C.R., Abramson, M.J., Benke, G., Martens, L., Joseph, W., 2018. Representativeness and repeatability of microenvironmental personal and head exposures to radio-frequency electromagnetic fields. Environ. Res. 162, 81–96. https://doi.org/10.1016/j.envres.2017.12.017.
Van Bladel, H., Stroobandt, B., Veludo, A.F., Deprez, K., Wiart, J., Röösli, M., Guxens, M., Joseph, W., Under revision. RF-EMF exposure assessment with add-on uplink exposure sensor in different microenvironments in seven European countries. Environ. Int.
Van Wel, L., Liorni, I., Huss, A., Thielens, A., Wiart, J., Joseph, W., Röösli, M., Foerster, M., Massardier-Pilonchery, A., Capstick, M., Cardis, E., Vermeulen, R., 2021. Radio-frequency electromagnetic field exposure and contribution of sources in the general population: an organ-specific integrative exposure assessment. J. Expo. Sci. Environ. Epidemiol. 31, 999–1007. https://doi.org/10.1038/s41370-021-00287-8.
Velghe, M., Joseph, W., Debouvere, S., Aminzadeh, R., Martens, L., Thielens, A., 2019. Characterisation of spatial and temporal variability of RF-EMF exposure levels in urban environments in Flanders, Belgium. Environ. Res. 175, 351–366. https://doi.org/10.1016/j.envres.2019.05.027.
Velghe, M., Aerts, S., Martens, L., Joseph, W., Thielens, A., 2021. Protocol for personal RF-EMF exposure measurement studies in 5th generation telecommunication networks. Environ. Health 20, 36. https://doi.org/10.1186/s12940-021-00719-w.
Veludo, A.F., Stroobandt, B., Van Bladel, H., Sandoval-Diez, N., Guxens, M., Joseph, W., Röösli, M., 2025. Exploring RF-EMF levels in Swiss microenvironments: an evaluation of environmental and auto-induced downlink and uplink exposure in the era of 5G. Environ. Res. 266, 120550. https://doi.org/10.1016/j.envres.2024.120550.
Vermeeren, G., Verloock, L., Aerts, S., Martens, L., Joseph, W., 2024. In situ assessment of uplink duty cycles for 4G and 5G wireless Communications. Sensors 24, 3012. https://doi.org/10.3390/s24103012.